NASA TECHNICAL NOTE

NASA TN D-3232

NASA TN D-3232

MECHANICAL PROPERTIES AND RECRYSTALLIZATION BEHAVIOR OF ELECTRON-BEAM-MELTED TUNGSTEN COMPARED WITH ARC-MELTED TUNGSTEN

by William D. Klopp and Walter R. Witzke

Lewis Research Center
Cleveland, Ohio

NATIONAL AERONAUTICS AND SPACE ADMINISTRATION • WASHINGTON, D. C. • JANUARY 1966

MECHANICAL PROPERTIES AND RECRYSTALLIZATION BEHAVIOR OF ELECTRON-BEAM-MELTED TUNGSTEN COMPARED WITH ARC-MELTED TUNGSTEN

By William D. Klopp and Walter R. Witzke

Lewis Research Center
Cleveland, Ohio

NATIONAL AERONAUTICS AND SPACE ADMINISTRATION

For sale by the Clearinghouse for Federal Scientific and Technical Information
Springfield, Virginia 22151 – Price $2.00

MECHANICAL PROPERTIES AND RECRYSTALLIZATION BEHAVIOR OF ELECTRON-BEAM-MELTED TUNGSTEN COMPARED WITH ARC-MELTED TUNGSTEN*

by William D. Klopp and Walter R. Witzke

Lewis Research Center

SUMMARY

A study has been conducted of the properties of tungsten fabricated from three ingots consolidated by electron-beam melting. The study included purity as a function of number of melts, recrystallization and grain growth behavior, low-temperature ductility, and high-temperature tensile and creep strength.

The level of most metallic impurities in tungsten decreased with increasing number of electron-beam melts, the reduction being greatest for aluminum, iron, nickel, and silicon. The levels of interstitial impurities generally were not affected by remelting. Resistivity ratios for single crystals machined from ingot slices tended to increase on remelting.

The recrystallization rates for worked, electron-beam-melted (EB-melted) tungsten were significantly higher than those observed earlier for arc-melted tungsten.

The grain growth rates of EB-melted tungsten were higher than those reported previously for arc-melted tungsten, further reflecting the higher purity of the EB-melted materials. The activation energies for both recrystallization and grain growth in EB-melted tungsten were consistent with expected values assuming grain boundary self-diffusion to be the rate-controlling reaction.

The ductile-brittle bend transition temperature for EB-melted tungsten is slightly higher in the worked condition than that reported for arc-melted tungsten. In the recrystallized conditions, the transition temperatures for EB- and arc-melted tungsten are similar.

The tensile strength of EB-melted tungsten at 2500° to 4000° F is less than that of arc-melted tungsten. This is partly associated with the large grain size of EB-melted tungsten. However, when compared at the same grain size,

---

*Presented in part in Effects of Grain Size on Tensile and Creep Properties of Arc-Melted and Electron-Beam-Melted Tungsten at 2250° to 4140° F by William D. Klopp, Walter R. Witzke, and Peter L. Raffo, AIME Trans., vol. 233, no. 10, Oct. 1965, pp. 1860-1866.

EB-melted tungsten is still about 15 percent weaker than arc-melted tungsten; this difference may be associated with the lower impurity levels in EB-melted tungsten.

The high-temperature creep strength of EB-melted tungsten is less than that of arc-melted tungsten, but this appears to be entirely the result of the larger grain size of EB-melted tungsten. When compared at similar grain sizes, the creep strengths of EB- and arc-melted tungsten at 3000° to 3500° F are similar.

Step-load creep tests at 2250° to 3630° F established that, at the stress levels studied (2130 to 6870 psi), EB-melted tungsten exhibits only transient creep behavior at 2250° to 2750° F. At 2875° F and higher, EB-melted tungsten exhibits transient creep initially, followed by steady creep and finally a period of accelerating creep rate terminating in failure. The activation energies for transient and steady creep are 106 400 and 141 000 calories per gram-mole, respectively. Recovery by dislocation climb is probably rate controlling during steady creep.

INTRODUCTION

In view of the potential usefulness of tungsten-base alloys as future high-temperature structural materials, base-line studies on tungsten consolidated by melting have been conducted at the NASA Lewis Research Center. A previous report (ref. 1) describes the metallurgical and mechanical properties of arc-melted tungsten; the present report describes the results of similar studies on electron-beam-melted (EB-melted) tungsten.

Although both arc melting and EB melting are conducted in high vacuum, there are important differences in the two processes. Normal arc-melting practice is to melt rather rapidly into a deep, nonretractable crucible. Chamber pressures range from 10^{-5} to 10^{-4} torr, although actual vapor pressures over the molten ingot top are higher because of the remoteness of the melting region. In contrast, EB melting is essentially a slow, drip-melting process. The ingot is formed on a stool that is retracted slowly during melting so that the molten ingot top is always at the top of the water-cooled crucible and is exposed to a chamber pressure of about 10^{-6} torr. Because of the slower melting rate, the longer hold time in the molten state, and the better vacuum above the molten metal, more purification through impurity volatilization can occur during EB melting than during arc melting. Further, it is general practice to EB-melt two or more times, thus effecting further purification. As a result of these differences, tungsten consolidated by EB melting is expected to be of higher purity than that consolidated by arc melting. The differences are difficult to detect analytically since the impurity levels are near the detection limits in both materials.

Previous studies on EB-melted tungsten have shown varying results regarding the ductile-brittle transition temperature. Witzke, et al. (ref. 2) found the tensile transition temperature for extruded EB-melted tungsten to be higher (790° F) than that for powder-metallurgy tungsten of similar grain size (640° F). However, Orehotsky and Steinitz (ref. 3) and Campbell and Dickinson (ref. 4)

showed that the tensile transition temperature for recrystallized wire drawn from zone-refined rod and EB-melted tungsten ingots was lower than that of powder-metallurgy wire and decreased with increasing melting time.

Additionally, limited studies have indicated that EB-melted tungsten has a lower recrystallization temperature and lower tensile strength at 600° to 3500° F (ref. 2) than less pure tungsten consolidated by powder-metallurgy techniques.

The purpose of the present study was to further characterize the properties of unalloyed EB-melted tungsten for comparison with the properties of powder-metallurgy and arc-melted tungsten and to provide base-line data for tungsten alloy studies. The properties evaluated included recrystallization behavior, grain growth behavior, low-temperature bend and tensile ductility, and high-temperature tensile and creep behavior.

SYMBOLS

A	temperature-dependent constant
a	exponential stress factor
b	exponential grain-size factor
C	circumference of circle, cm
c	constant
e	creep strain
$\dot{e}$	steady creep rate, sec^{-1}
f	grain shape factor (=1)
G	boundary migration rate, cm/sec
G_o	frequency factor for boundary migration, cm/sec
K	parabolic grain growth rate, cm^2/sec
K'	transient creep rate, $(sec^{-1})(psi^{-10.2})$
k	steady creep constant
L	average grain diameter, cm
L_o	initial average grain diameter, cm
M	magnification
$\bar{N}$	average number of grains per unit volume, cm^{-3}

$\bar{N}_o$ average number of recrystallization nuclei per unit volume, cm^{-3}

n number of intercepts

Q activation energy, cal/(g)(mol)

R gas constant, cal/(mol)(^oK)

S engineering stress, psi

T temperature, ^oK

T_m absolute melting point

t time, sec

UTS ultimate tensile strength, psi

X fraction recrystallized

β transient creep constant, $sec^{-1/3}$

ϵ true plastic strain

σ true stress, psi

σ_o extrapolated stress intercept at zero strain, psi

χ strain-hardening coefficient, psi^2

EXPERIMENTAL PROCEDURES

Starting Materials

The starting materials for this study consisted of sintered unalloyed (undoped) 15- to 18-pound tungsten bars. These bars measured 1.125 to 1.1875 inches in diameter by 24 inches long and were approximately 93 percent dense.

Melting

The three ingots employed for the major portion of this study were consolidated by EB melting under a vacuum of 10^{-6} torr into a water-cooled copper crucible equipped with a retractable stool (ref. 2). A remote, magnetically focused EB-melted gun was employed for initial melting of the sintered bar, since gases evolved from the bar during melting caused considerable splattering and promoted electrical instability of the beam. The tungsten starting material was fed horizontally into the electron beam just above the crucible and melted rapidly (0.5 to 1 lb/min) to give a 1.5-inch-diameter ingot. This ingot was then remelted slowly (0.1 to 0.2 lb/min) using a circumferential "close" gun. The ingot was fed vertically through the close gun and melted into a 2.5-inch-

TABLE I. - CHEMICAL ANALYSES OF ELECTRON-BEAM-MELTED TUNGSTEN INGOTS

Element	EB-melted ingots			Arc-melted ingots[a]
	EB-43 (7 melts)	EB-87 (4 melts)	EB-100 (7 melts)	
	Impurity content, ppm[b]			
Oxygen	[c]3	2	2	6
Nitrogen	[c]10	13	<5	10
Carbon	[c]7	4	10	6
Hydrogen	[c]<1	<1	--	<1
Aluminum	.16	.13	.05	6.3
Calcium	1	<.05	.02	---
Chromium	.48	.64	1.6	<3
Cobalt	.015	<.1	.015	---
Columbium	<.5	<.5	2.5	---
Copper	2.8	.07	.27	1.2
Iron	.19	.07	.11	16
Magnesium	.05	<.01	.08	---
Manganese	<.01	<.01	.02	---
Molybdenum	<1	2.8	1	11
Nickel	.02	<.1	.08	2.1
Silicon	1.5	.38	.95	8.4
Sodium	.1	<.01	<.005	<5
Tantalum[c]	32	6	9	---
Titanium	<.1	<.1	.008	---

[a]Average analysis of 5 lots of fabricated tungsten from ref. 1.

[b]Analyses conducted as follows:
Oxygen and hydrogen - vacuum fusion
Nitrogen - Kjeldahl
Carbon - combustion
Metallics - average of emission and mass spectrography. Only elements detected by both emission and mass spectrography are reported.

[c]Analyses on fabricated materials.

diameter crucible.

The number of melts for the three ingots used in the present study was four or seven, as shown in table I. A fourth ingot, EB-175, was also melted seven times and evaluated for melting effects on purity only.

Extrusion

Two of the three ingots (EB-43 and EB-100) were machined into billets measuring 2.08 inches in diameter by 4.5 inches tall and extruded in a hydraulic extrusion press. The third ingot, EB-87, was machined into a billet measuring 1.70 inches in diameter by 2.5 inches long and extruded in an impact extrusion press. The surface quality of all three extrusions was good. All extrusions were sound and could be fabricated into good quality rod and/or sheet.

Variations in the preheat temperature between 3000° and 3500° F, reduction ratios between 6 and 8, or in the type of extrusion press did not appear to significantly affect the surface quality of the extrusion.

Fabrication

After sectioning to obtain metallographic and analytical specimens, the extruded rods were warm fabricated to rod and/or sheet to provide material for recrystallization and grain growth studies and bend, tensile, and creep tests. Swaging and rolling were conducted at a starting temperature of 2300° F and a finishing temperature of 2100° F.

Recrystallization and Grain Growth Studies

Recrystallization studies were conducted on swaged rod from lot EB-43 and on both rod and sheet from lot EB-100. Rod specimens were 0.22 or 0.36 inch in diameter by 0.25 inch long, while sheet specimens were 0.026 to 0.056 inch thick, 0.25 inch wide, and 0.375 inch long. These specimens were annealed for times ranging from 10 minutes (0.13 hr) to 7 hours at temperatures from 1900° to 2700° F. All annealing treatments were conducted in an induction-heated hydrogen-atmosphere furnace. Temperatures were monitored with a

tungsten/tungsten-26 percent rhenium thermocouple.

Longitudinal sections of the annealed specimens were examined metallographically and the fraction recrystallized was averaged from visual estimates by two observers over at least 10 areas on each specimen. The average grain diameter was determined for specimens recrystallized 90 percent or more by counting the number of boundary intercepts with a circle 48.3 centimeters in circumference on a projection screen. The relation employed for calculating the grain diameter was

$$L = \frac{C}{Mn} \tag{1}$$

At least five counts of about 40 intercepts each were averaged for each specimen. The number of grains per cubic centimeter is calculated (ref. 5) as

$$\overline{N} = \left(\frac{1}{L}\right)^3 \tag{2}$$

Grain growth studies were also conducted on a 0.36-inch-diameter rod (EB-43 and EB-100) or 0.045-inch-thick sheet (EB-87) specimens from each of the three lots. These specimens were annealed for 1 or 4.5 hours at temperatures ranging from 2500° to 4200° F. Annealing treatments at 2500° to 3000° F were conducted in the induction-heated hydrogen-atmosphere furnace used for recrystallization studies. Annealing treatments at higher temperatures were conducted in a resistance-heated tungsten-element vacuum furnace. Temperatures in the latter furnace were measured by optical pyrometry and are estimated to be accurate to ±25° F. The initial condition for grain growth study specimens was as worked; the initial grain size was taken as that which was characteristic of the same material immediately after recrystallization. Final grain sizes after annealing were determined by the intercept-count method described previously.

Bend Transition Studies

Bend specimens measuring 0.375 by 0.75 inch were cut from 0.050-inch-thick sheet rolled from extruded bar of lot EB-87. Prior to testing, the bend specimens were electropolished for 10 minutes at 12 volts direct current in a 2 percent sodium hydroxide aqueous solution. This treatment removed 3 to 6 mils of material per side and produced smooth, scratch-free surfaces on the specimens. Bend tests were conducted in a specially constructed apparatus as described in reference 1. The bend radius was four times the specimen thickness (4T).

Tensile and Creep Studies

Tensile specimens for both low- and high-temperature tensile creep tests were machined from 0.36-inch-diameter swaged rod. The specimen reduced section was 0.16 inch in diameter by 1.03 inches long.

For low-temperature testing to determine the ductile-brittle transition

temperature, the specimen surfaces were electropolished in the sodium hydroxide solution described previously. This procedure has been shown to improve the reproducibility of tensile ductility data and also to lower the ductile-brittle transition temperature slightly by reducing surface roughness. Testing was conducted in vacuum at a crosshead motion rate of 0.005 inch per minute to about 0.5 percent plastic strain in order to define the 0.2 percent offset yield strength, after which the crosshead movement rate was increased to 0.05 inch per minute to fracture.

Tensile tests at 2500° to 4000° F were conducted on a screw-driven tensile machine equipped with a high-temperature vacuum (1×10^{-5} torr) furnace, which has been described previously (ref. 6). Crosshead movement rates were the same as those employed for low-temperature testing. Approximate true-stress - true-strain flow curves were constructed for each tensile test up to the point of maximum load by assuming constant volume and uniform deformation in the reduced section. Specimen extension during testing was taken as equal to the crosshead movement since extensometers capable of accurate strain measurements at 2500° to 4000° F were not available. This use of strain measurements based on crosshead movement introduces some error since crosshead motion also reflects grip settling and creep during testing.

Creep tests were conducted in a conventional beam-load machine equipped with a vacuum chamber and tantalum heater similar to that used for tensile testing. Pressure during testing was maintained at approximately 10^{-6} torr. Specimen extensions were measured from loading rod movement and corrected for creep of the loading rods. Calibrated tungsten/tungsten-26 percent rhenium thermocouples tied to the center of the specimen reduced section were employed for temperature measurements during testing.

Grain sizes were measured in the heated but undeformed shoulders of all tensile and creep specimens after testing.

RESULTS AND DISCUSSION

Effect of Electron-Beam Melting on Purity

Chemical analyses of the three ingots of EB-melted tungsten before fabrication are shown in table I (p. 5). The spectrographic analyses for metallic impurities are averages of emission and mass spectrographic analyses.

The oxygen contents of these materials are seen to be consistently lower than the average for five other lots of arc-melted tungsten from reference 1. Nitrogen and carbon contents, however, vary from lot to lot and are similar to those observed for the arc-melted materials.

Spectrographic analyses indicate that small amounts of tantalum were present in the fabricated materials. The tantalum contents ranged from 6 to 32 ppm, while tantalum was undetected in the arc-melted materials. This contamination apparently resulted from melting onto tantalum-10 percent tungsten melting pads, but at these levels did not appear to significantly affect the properties of EB-melted tungsten.

The levels of metallic impurities, other than tantalum, were lower in the EB-melted materials than in the arc-melted materials. As seen in table I (p. 5), the levels of aluminum, iron, nickel, and silicon in particular, were much lower in the EB-melted tungsten than in arc-melted tungsten. Although the analyses show considerable scatter, it appears that the major effect of EB melting is to reduce the levels of metallic impurities without significantly affecting the amounts of interstitial impurities.

The effect of remelting on ingot purity was studied on ingot EB-175, which was not included in other evaluations. Chemical analyses were obtained after remote gun melting, close gun melting, and after each subsequent close gun remelt. In addition, as a further indication of purity, electrical resistivity ratios (resistivity at 4.2° K/resistivity at 300° K) were determined on single crystals, which were spark discharge machined from individual grains of ingot EB-175 after each melt. This ingot was melted onto a large-grained tungsten pad in order to promote the growth of large columnar grains and to eliminate the tantalum contamination associated with melting directly on the tantalum-10 percent tungsten retractable stool.

Results of the chemical analyses and resistivity ratio determinations are

TABLE II. - CHEMICAL ANALYSES AND RESISTIVITY RATIOS

ON INGOT EB-175 AFTER EACH MELT

Element	Remote gun consolidation melt	Close gun melt	Third melt	Fourth melt	Fifth melt	Sixth melt	Seventh melt
	Analysis, ppm[a]						
Oxygen	1	5	3	1	2	2	8
Nitrogen	5	13	10	7	9	7	7
Carbon	5	25	5	5	5	5	33
Aluminum	1.7	<.1	2.5	1.5	.1	.2	.5
Calcium	1.7	.6	.4	.9	1.7	.15	.25
Chromium	.5	.7	.6	.15	.2	.2	.2
Columbium	.1	1.7	<.1	.1	<.1	<.1	.1
Copper	1	<.1	2.1	.25	.5	.7	.5
Iron	.25	.3	<.1	.03	.1	.1	.15
Molybdenum	5	2.8	5	4	4	<.01	<.01
Nickel	.08	.2	.05	.01	.2	.02	.05
Silicon	20	1.3	12	15	1.3	.3	1
Tantalum	.1	3.5	7	12	5	4	<3
	Resistivity ratio[c]						
	----	[b]734	1130	2450	2500	1800	2930

[a]Analyses for metallics are average of analyses by mass and by emission spectrography.

[b]Specimen was determined after testing to be polycrystalline; all others were single crystals.

[c]Ratio of electrical resistivity at 4.2° K to that at room temperature.

given in table II. Although both the chemical analyses and resistivity ratio data show considerable scatter, a trend toward higher purity with repeated remelting is apparent. The highest electrical resistivity ratio observed here, 2930, is considerably lower than the values of 40 000 and 70 000 observed by Koo (ref. 7) and Drangel and Murray (ref. 8), respectively, for tungsten single crystals grown by the floating zone melting technique. This difference may be associated either with lower purity or with a larger amount of substructure in the present materials.

Recrystallization Behavior

Recrystallization studies were conducted on rod from EB-43 and on both rod and sheet from EB-100 in order to determine the variations in behavior between lots and the effects of variations in prior strain, time, and temperature of annealing. It was also of interest to compare the annealing response of high-purity EB-melted tungsten with that of the less pure arc-melted tungsten described in reference 1. Data from the present studies are presented in table III. Micrographs of representative partially and fully recrystallized structures (EB-100) are included in figure 1.

The effects of varying prior strain were studied to a limited extent. The EB-43 material recrystallized faster for a prior reduction of 59 percent as compared to a prior reduction of 46 percent. The grain size of the more heavily reduced material was finer after recrystallization than that of the less heavily reduced material, as would be expected. Lot EB-100 exhibited similar behavior, although there was more scatter in these data.

In order to compare more quantitatively the recrystallization behavior of the various lots, the data were correlated in terms of a nucleation and growth transformation by the Johnson-Mehl relation (ref. 9)

$$X = 1 - e^{-f\overline{N}_o G^3 t^3} \tag{3}$$

The form of this relation as here employed assumes that, at the start of recrystallization, a number of high-strain energy sites $\overline{N}_o$ transform relatively rapidly into new strain-free grain nuclei. These nuclei then grow, the driving force being equal to the difference in potential strain energy between the strained unrecrystallized material and the unstrained recrystallized material. The boundaries of the new strain-free grains move linearly with time at a temperature-dependent rate G until they impinge on boundaries from other new strain-free grains. At this point, boundary migration ceases. There is little tendency for small grains to be consumed by larger grains at these temperatures because the differences in energy between a small grain and a large grain (associated with the differences in radii of curvature of the grain boundaries) are small compared with the energy differences between the strained and unstrained areas. For this reason, the number of nuclei $\overline{N}_o$ has been taken in this study to be equal to the number of recrystallized grains per cubic centimeter for the calculation of G, the boundary migration rate.

TABLE III. - RECRYSTALLIZATION BEHAVIOR OF UNALLOYED ELECTRON-BEAM-MELTED TUNGSTEN

Material geometry	Reduction during fabrication, percent[c]	Initial average grain diameter, L_o, cm (a)	Average number of recrystallization nuclei per unit volume, $\bar{N}_o$, cm^{-3} (b)	Annealing condition: Time, hr	Annealing condition: Temperature, °F	Fraction recrystallized, X	Hardness, VHN[d]	Average grain diameter, L, cm	Boundary migration rate, G, cm/sec
Lot EB-43									
0.36-inch rod	46	0.0229	8.35×10^4	As swaged		----	455	------	----------
				0.17	2100	0	444	------	----------
				3	↓	.02	455	------	0.547×10^{-6}
				5		.34	421	------	.945
				7		.61	405	------	.903
				1.5	2200	.02	468	------	1.47
				2.5	2200	.26	387	------	1.72
				3.5	2200	.86	---	------	2.29
				.17	2300	.04	422	------	13.6
				.25	↓	.02	435	------	6.96
				.50		.12	437	------	6.34
				.75		.03	428	------	2.65
				.17	2500	.94	416	0.0265	53.2
				.33	2500	.98	363	.0208	30.1
				1.0	2500	1.00	374	.0232	----------
				.17	2700	1.00	347	.0210	----------
	59	0.0176	1.83×10^5	As swaged		----	455	------	----------
				0.17	1900	0	467	------	----------
				.17	2100	0	435	------	----------
				3	↓	.03	455	------	0.514×10^{-6}
				5		.76	429	------	1.10
				7		.53	442	------	.637
				1.5	2200	.25	437	------	2.15
				2.5	2200	.88	370	------	2.50
				3.5	2200	.99	354	0.0198	1.71
				.17	2300	.25	435	------	19.3
				.25	↓	0	440	------	----------
				.50		.49	380	------	8.60
				.75		.35	368	------	4.92
				.17	2500	.95	369	.0185	42.5
				.17	2500	1.00	---	.0139	----------
				.33	2500	1.00	360	.0160	----------
				.17	2700	1.00	333	.0200	----------
Lot EB-100									
0.22-inch rod	63	0.0190	1.45×10^5	0.58	2200	0.13	446	------	4.70×10^{-6}
				.70	↓	.33	413	------	5.52
				.85		.49	401	------	5.41
				1.20		.65	380	------	4.46
				1.47		.70	387	------	3.83
				1.73		.90	354	------	4.00
				1.0	2300	1.00	---	0.0190	----------
	83	0.0220	9.42×10^4	0.5	2300	0.46	409	------	32.5×10^{-6}
				1.0	2300	.73	421	------	9.7
				2.0	2300	1.00	348	0.0228	----------
				.13	2400	.75	394	------	74.2
				.20	↓	.66	394	------	45.5
				.27		.61	413	------	32.8
				1.0	↓	1.00	360	.0211	----------
	89	0.0130	4.55×10^5	0.20	2200	0.62	401	------	17.8×10^{-6}
				.25	↓	.71	387	------	15.5
				.30		.72	373	------	13.0
				.35		.88	394	------	13.2
				.42		.93	373	------	11.9
				1.0	2300	1.00	---	0.0144	----------
				1.0	2400	1.00	---	.0116	----------
0.056-inch sheet	93.6	0.00513	7.41×10^6	1	2000	0.65	425	------	1.45×10^{-6}
					2100	1.00	383	0.00513	----------
0.040-inch sheet	95.4	0.00441	1.17×10^6	1	2000	0.88	394	-------	1.57×10^{-6}
					2100	1.00	373	0.00441	----------
0.026-inch sheet	97	0.00400	1.56×10^7	1	2000	0.94	351	-------	3.95×10^{-6}
					2100	1.00	360	0.00400	----------

[a]Averaged from measurement on just-recrystallized specimens.
[b]Calculated from initial average grain diameter by eq. (2).
[c]Reduction after extrusion or intermediate recrystallizing anneal.
[d]10-kg load.

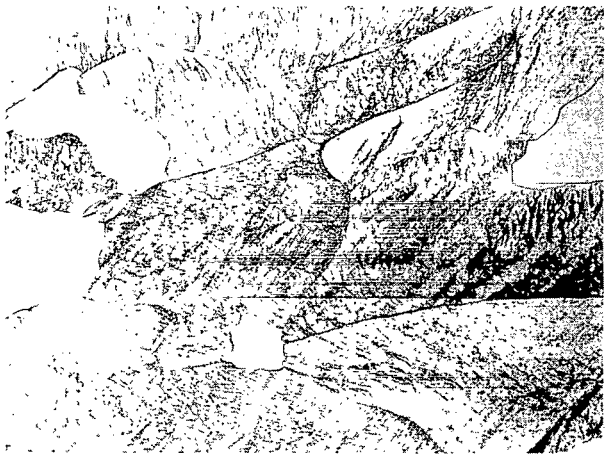

(a) Annealed for 1/2 hour at 2300° F; 46 percent recrystallized.

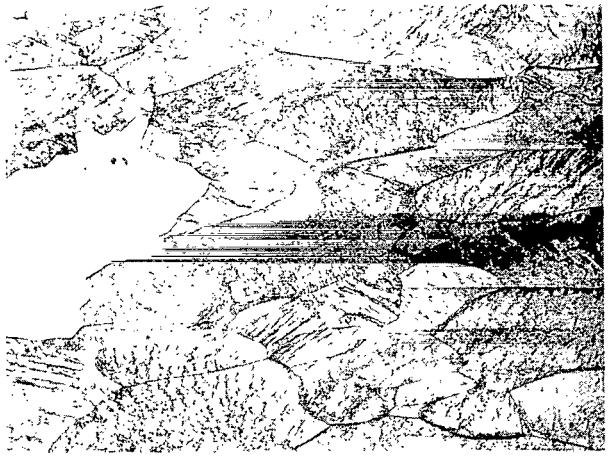

(b) Annealed for 1 hour at 2300° F; 73 percent recrystallized.

(c) Annealed for 1 hour at 2400° F; fully recrystallized; average grain diameter, 0.0211 centimeter.

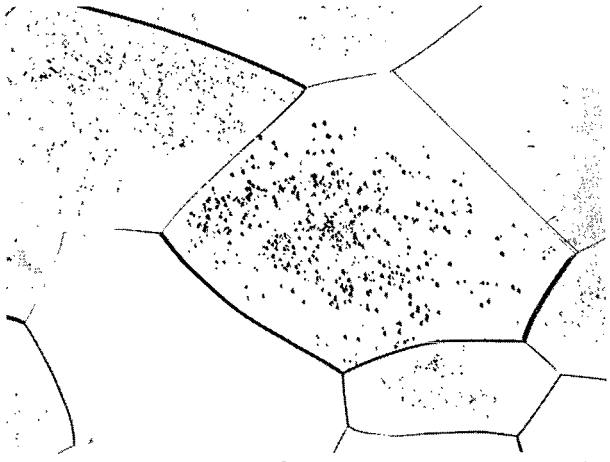

(d) Annealed for 1 hour at 2800° F; fully recrystallized; average grain diameter, 0.0321 centimeter.

(e) Annealed for 1 hour at 3200° F; fully recrystallized; average grain diameter, 0.0731 centimeter.

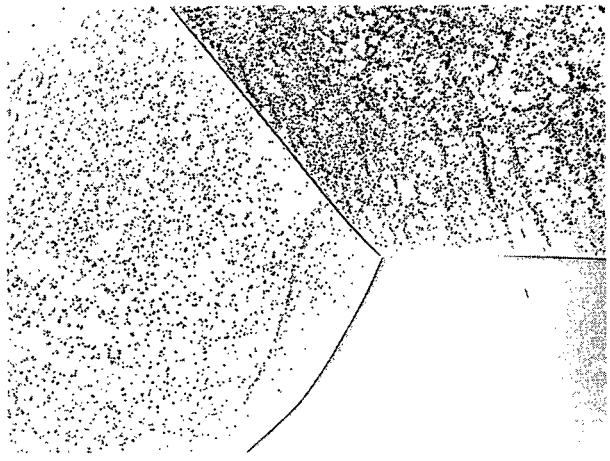

(f) Annealed for 1 hour at 3600° F; fully recrystallized; average grain diameter, 0.2147 centimeter.

Figure 1. - Recrystallization and grain growth of extruded and swaged electron-beam-melted tungsten (lot EB-100); X100.

More recent studies have suggested that certain of the assumptions basic to the Johnson-Mehl relation may not be strictly correct. For example, in reference 10 it was concluded, based on studies of silicon iron, that the rate of boundary migration G decreased with time rather than remaining constant. This was attributed to a segregation of the solute to subgrain boundaries in the unrecrystallized material. Detert and Dressler (ref. 11), working with high-purity nickel, observed a time dependency of $t^{1.4}$ rather than t^3 as in the Johnson-Mehl relation. For the purposes of the present study and in view of the data scatter obtained, the use of the Johnson-Mehl relation appears adequate.

Values for the number of recrystallization nuclei $\overline{N}_O$ and the calculated boundary migration rates G are included in table III and are averaged in table IV for the various temperatures and reductions studied. It is seen that the calculated values of G vary only slightly with annealing time (table IV) and, for EB-43, with prior reduction. For EB-100, the very limited data suggest that G increases with increasing prior reduction, but, in view of the results for EB-43 and for arc-melted tungsten (ref. 1), this trend is attributed to data scatter. Thus, the recrystallization behavior of each lot may be semiquantitatively described in terms of the number of recrystallization nuclei $\overline{N}_O$, which is a function of prior strain, and the rate of strain-induced grain boundary migration G, which varies with temperature.

The average boundary migration rates for both lots studied are included in table IV and are plotted in figure 2, along with similar data for arc-melted

TABLE IV. - AVERAGE RECRYSTALLIZATION RATES FOR

ELECTRON-BEAM-MELTED TUNGSTEN

Lot	Temperature, °F	Reduction, percent	Logarithmic average of boundary migration rate for each reduction, cm/sec	Logarithmic average of boundary migration rate for each lot, cm/sec
EB-43	2100	46 59	7.76×10^{-7} 7.12	7.43×10^{-7}
	2200	46 59	1.80×10^{-6} 2.09	1.94×10^{-6}
	2300	46 59	6.31×10^{-6} 9.35	7.47×10^{-6}
	2500	46 59	4.00×10^{-5} 4.25	4.08×10^{-5}
EB-100	2000	93.6 95.4 97	1.45×10^{-6} 1.57 3.95	2.08×10^{-6}
	2200	63 89	4.61×10^{-6} 1.41×10^{-5}	7.67×10^{-6}
	2300	83	1.78×10^{-5}	1.78×10^{-5}
	2400	83	4.80×10^{-5}	4.80×10^{-5}

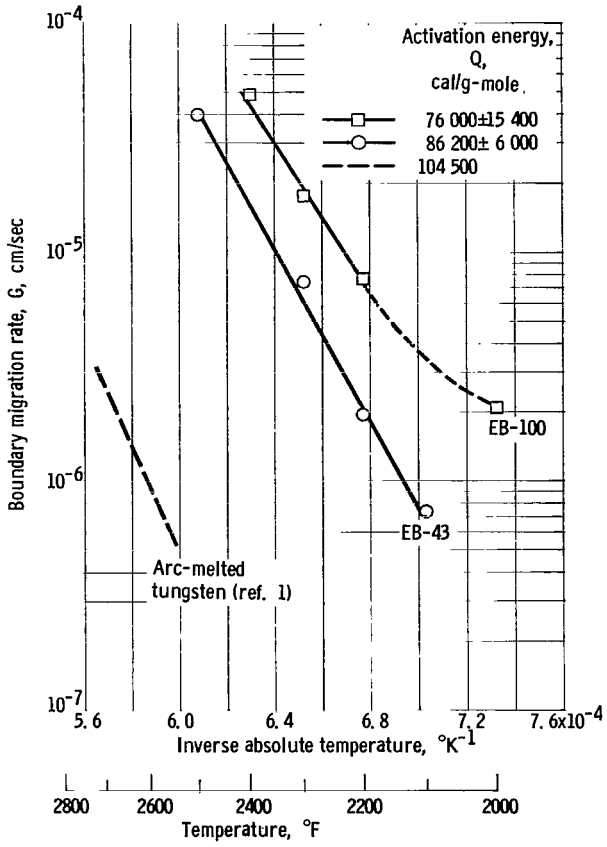

Figure 2. - Temperature dependence of strain-induced boundary migration rates of electron-beam- and arc-melted tungsten.

tungsten. It is seen that the boundary migration rates for the high-purity EB-melted material are significantly higher than those for the less pure arc-melted tungsten.

The temperature dependency of G may be expressed by

$$G = G_o e^{-Q/RT} \qquad (4)$$

Values for the activation energy Q were calculated by a least-squares analysis and are 76 000±15 400 for EB-100 and 86 200±6 000 calories per gram-mole for EB-43. These values lie well within the range of activation energies estimated for the grain boundary self-diffusion of tungsten, 61 000 to 107 000 calories per gram-mole. The latter values were estimated based on 0.4 to 0.7 of the activation energy for volume self-diffusion (refs. 12 and 13) of tungsten, which has recently been determined as 153 100 calories per gram-mole (ref. 14). The activation energies for recrystallization of EB-melted tungsten are significantly lower than the values of 104 500 and 100 000 calories per gram-mole observed for arc-melted and powder-metallurgy tungsten, respectively (refs. 1 and 15), possibly reflecting the higher purity of EB-melted tungsten.

Grain Growth Behavior

The grain growth behavior of the three lots was studied by annealing worked specimens from each lot for 1 hour at temperatures ranging from 2500° to 4200° F. The average grain diameters after annealing are given in table V.

To facilitate comparison of the behaviors of the various lots, it was assumed that grain growth was ideal and not impeded by precipitates or internal voids. Grain growth under these conditions may be expressed as (ref. 16):

$$L^2 - L_o^2 = Kt \qquad (5)$$

This relation was used to calculate values of K for each annealing treatment by assuming L_o equal to the just-recrystallized grain diameter measured during the recrystallization studies. Values for K and L_o are included in table VI, and a plot of log K against inverse temperature is shown in figure 3.

TABLE V. - GRAIN GROWTH BEHAVIOR OF ELECTRON-BEAM-MELTED TUNGSTEN

Material geometry	Initial average grain diameter, L_o, cm	Reduction, percent	Annealing condition		Average grain diameter, L, cm	Grain growth rate, K, cm^2/sec
			Time, hr	Temperature, °F		
Lot EB-43						
0.36-inch rod	0.0229	46	4.5	3000	0.0280	0.016×10^{-6}
			1	3100	.0294	.0944
			↓	3300	.0370	.235
				3400	.0485	.508
				3500	.0738	1.37
				3700	.128	4.41
				4000	.127	4.33
				4000	.420	48.9
	0.0176	59	1	3100	0.0252	0.0903×10^{-6}
			↓	3300	.0321	.200
				3500	.142	5.52
				3600	.0644	1.07
				3800	.246	16.7
				4000	.321	28.5
Lot EB-87						
0.045-inch sheet	0.00424	85	1	3000	0.00991	0.0223×10^{-6}
			↓	3500	.0338	.312
				3800	.0713	1.41
				4000	.118	3.86
				4200	.104	3.00
Lot EB-100						
0.36-inch rod	0.0220	83	1	2500	0.0263	0.0575×10^{-6}
			↓	2500	.0363	.232
				2600	.0317	.145
				2800	.0321	.152
				3000	.0430	.379
				3200	.0731	1.35
				3400	.0862	1.93
				3600	.185	9.35
				3600	.215	12.7
				3600	.349	33.7

TABLE VI. - LOW-TEMPERATURE TENSILE PROPERTIES OF ELECTRON-BEAM-MELTED TUNGSTEN

Annealing condition		Average grain diameter, L, cm	Test temperature, °F	0.2 Percent offset yield strength, psi	Ultimate tensile strength, UTS, psi	Elongation, percent	Reduction in area, percent
Time, hr	Temperature, °F						
			Lot EB-43				
As swaged (46 percent)		(a)	510	73 900	82 100	2.0	1.2
			550	73 000	80 200	18.9	53.5
			615	67 200	71 500	16.6	64.7
As swaged (59 percent)		(a)	405	86 000	101 200	2.3	3.0
			470	81 700	92 700	13.1	44.8
			500	77 800	86 700	15.6	55.5
			590	74 400	80 000	16.8	70.3
			700	72 500	74 400	----	79.5
0.17	[b]1900	(a)	415	89 400	101 700	1.9	0.8
			470	76 600	87 000	18.6	54.8
			600	71 800	76 600	10.9	66.4
	[b]2100	(a)	400	86 300	97 600	1.3	0
			445	80 200	91 600	2.9	2.7
			500	72 600	82 800	21.9	56.8
	[b]2300	(a)	460	------	78 500	4.4	2.4
			485	55 700	74 600	12.4	9.9
			510	73 100	83 000	16.5	48.6
	[b]2500	0.0139	475	30 700	46 200	3.1	1.5
			500	41 100	66 100	17.5	35.2
			550	25 400	56 000	31.1	48.4
1	[c]2500	0.0232	600	13 900	51 700	37.8	36.0
			695	11 800	47 900	22.7	18.3
			695	8 820	48 400	24.8	19.2
			810	16 500	45 200	38.5	70.9
4.5	[c]3000	0.0280	590	[d]18 400	44 600	9.4	8.5
			650	[d]17 500	47 800	40.2	61.5
			650	[d]17 600	47 900	41.2	53.5
			700	[d]8 830	45 700	42.1	62.7
			705	[d]16 300	48 200	39.4	43.5
1	[c]3400	0.0485	605	11 100	47 300	28.2	20.2
			665	8 000	44 800	38.2	42.0
			750	6 820	42 100	48.6	58.9
	[c]3700	0.128	495	23 900	51 500	23.1	36.6
			590	[d]15 700	45 400	42.7	54.0
			700	9 540	38 300	27.4	67.8
	[c]4000	0.127	315	49 100	84 500	3.6	8.8
			500	28 400	52 700	2.0	3.6
			555	14 600	36 400	21.6	100.0
			Lot EB-100				
As swaged (83 percent)		(a)	395	86 600	98 900	7.4	4.4
			470	74 200	84 900	11.2	32.7
			530	64 500	73 500	13.4	50.5
			575	67 600	74 600	12.9	56.4
1	2500	0.0263	705	7 910	44 300	26.5	23.6
			755	7 060	42 900	36.1	40.0
			805	13 700	40 000	37.5	63.9

[a]Worked microstructure.
[b]Swaged to 59 percent reduction.
[c]Swaged to 46 percent reduction.
[d]Specimen exhibited yield point drop; lower yield point reported.

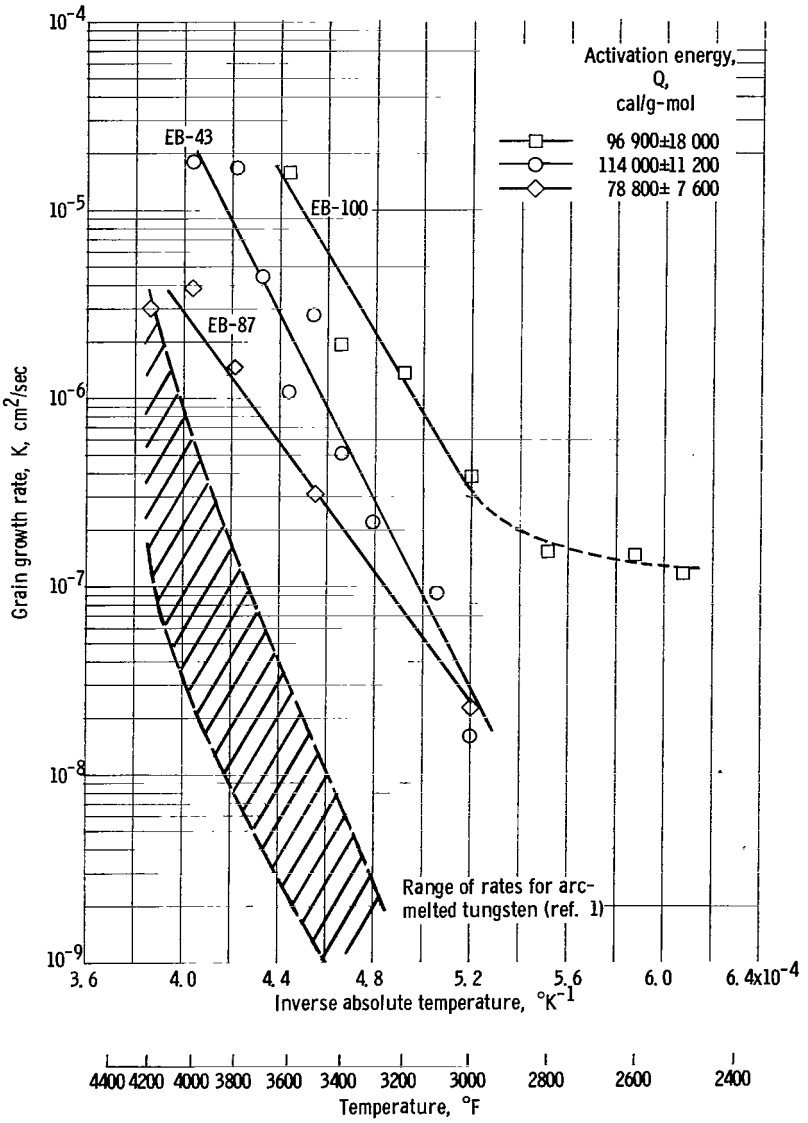

Figure 3. - Grain growth rates of electron-beam-melted tungsten.

All of the lots of EB-melted tungsten showed higher rates of grain growth than the arc-melted tungsten studied in reference 1. The micrographs of EB-melted tungsten (lot EB-100) after high-temperature annealing, shown in figure 1 (p. 11), indicate no observable tendency towards discontinuous grain growth, which if present would suggest the presence of insoluble impurities.

The activation energies corresponding to the slopes of the lines in figure 3 are seen to range from 78 800±7 600 to 114 000±11 200 calories per gram-mole. Although the latter of these values is slightly above the estimated upper limit for the activation energy for grain boundary diffusion, this process is considered to be the rate-determining reaction during grain growth.

Ductile-Brittle Tensile Transition Behavior

Tensile properties of lots EB-43 and EB-100 were measured at temperatures ranging from 315° to 810° F in order to define the ductile-brittle tensile transition temperature after various annealing treatments. Data for these tests are given in table VI and are summarized in table VII. Figure 4 shows a plot of reduction in area against test temperature for material from lot EB-43 after various annealing treatments.

The data in table VII show that tungsten from lot EB-43 follows the usual pattern of decreasing transition temperature with increasing prior work. Materials with 46 and 59 percent prior work had as swaged transition temperatures of 530° and 460° F, respectively. Stress-relief annealing for 10 minutes at 1900° to 2500° F affected the transition temperature of the 59 percent swaged materials from lot EB-43 only slightly.

The recrystallized materials did not follow the expected pattern of increasing transition temperature with increasing grain size. Instead the data indicate that the highest transition temperatures are associated with the fine-grained just-recrystallized materials, and annealing at higher temperatures substantially reduces the transition temperature. The 46 percent swaged material from lot EB-43 actually showed lower transition temperatures after annealing at 3700° and 4000° F (510° and 525° F, respectively) than in the as swaged condition (530° F). These large-grained specimens exhibited a chisel-type fracture. In contrast, annealing for 1 hour at 2500° F to a fine-grained recrystallized structure raised the transition temperatures for materials from lots EB-43 and EB-100 to 740° and 755° F, respectively.

The tensile transition temperatures for the EB-melted materials are comparable to those obtained for arc-melted materials in a previous study (ref. 1).

Ductile-Brittle Bend Transition Behavior

Bend transition temperatures were determined on 40-mil sheet from EB-87 tungsten and one lot of arc-melted tungsten. The arc-melted tungsten, lot A-73, was consolidated from the same lot of commercially prepared electrodes as lot EB-87. Both were fabricated similarly so that any differences in bend

TABLE VII. - TENSILE TRANSITION TEMPERATURES

FOR ELECTRON-BEAM-MELTED TUNGSTEN

Lot	Annealing condition		Average grain diameter, L, cm	Ductile-brittle transition temperature,[a] °F
	Time, hr	Temperature, °F		
EB-43	As swaged (46 percent)		(b)	530
	As swaged (59 percent)		(b)	460
	0.17	[c]1900	(b)	445
	↓	[c]2100	(b)	480
		[c]2300	(b)	485
		[c]2500	0.0139	505
	1	[d]2500	.0232	740
	4.5	[d]3000	.0280	630
	1	[d]3400	.0485	660
	1	[d]3700	.128	510
	1	[d]4000	.127	525
EB-100	As swaged (83 percent)		(b)	490
	1	2500	0.0263	755

[a]That temperature where reduction in area is 40 percent, which is approximately one-half its maximum value.

[b]Worked microstructure.

[c]Swaged to 59 percent reduction.

[d]Swaged to 46 percent reduction.

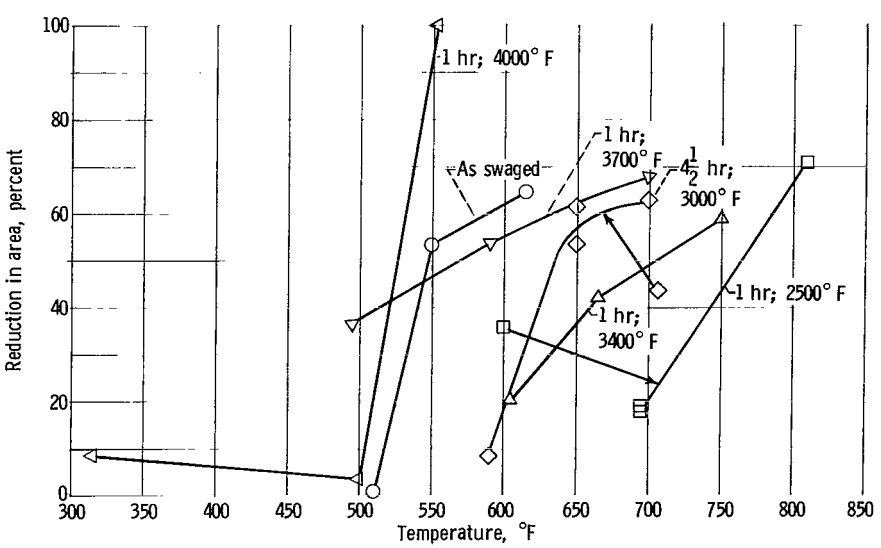

Figure 4. - Low-temperature tensile ductility of electron-beam-melted tungsten after various annealing treatments (lot EB-43).

TABLE VIII. - BEND TRANSITION TEMPERATURES FOR

ELECTRON-BEAM- AND ARC-MELTED TUNGSTEN

Lot	Annealing condition		Average grain diameter, L, cm	Sheet thickness, mils	Bend radius to thickness ratio	Bend transition temperature, °F
	Time, hr	Temperature, °F				
EB-87	As rolled		(a)	40	4	285
	1	1900	(a)	40	4	350
		2000	(a)	↓	↓	550
		2100	(a)			525
		2200	0.00424			525
		3000	.00991			655
		3500	.0338			750
		3800	.0713			705
		4000	.118			695
		4200	.104			630
A-73	As rolled		(a)	40	4	200
	1	2000	(a)	40	4	< 250
		2200	↓	↓	↓	250
		2400				325
		2600				400
		2800	0.00236			500
		3000	.00268			580
		3500	.00455			690
		3800	.00764			655
		4000	.0157			660
		4200	.0327			660

[a]Worked microstructure.

transition behavior could be related to the differences between the two melting processes. Bend transition data for both of these materials after various annealing treatments are presented in table VIII. The bend transition temperatures of lots EB-87 and A-73 are plotted as a function of annealing temperature in figure 5, which also includes data on powder-metallurgy tungsten (ref. 17) for comparison.

It is seen from the data in table VIII that the bend transition temperatures for as rolled EB-melted tungsten (lot EB-43) is 285° F, while that for the arc-melted material was slightly lower, 200° F. Annealing EB-melted tungsten at 1900° F increased the transition temperature slightly. Recrystallization was evident after annealing for 1 hour at 2000° to 2200° F and was accompanied by an increase in the transition temperature as high as 525° to 550° F. Annealing at higher temperatures, 3000° to 3500° F, further increased the transition temperatures to about 700° F.

Comparison of the bend transition temperatures for sheet from lots EB-87 and A-73, shown in figure 5, shows that after annealing for 1 hour at 1900° to 2200° F, the EB-melted material has a significantly higher transition temperature than the arc-melted tungsten. This is attributed to the lower recrystal-

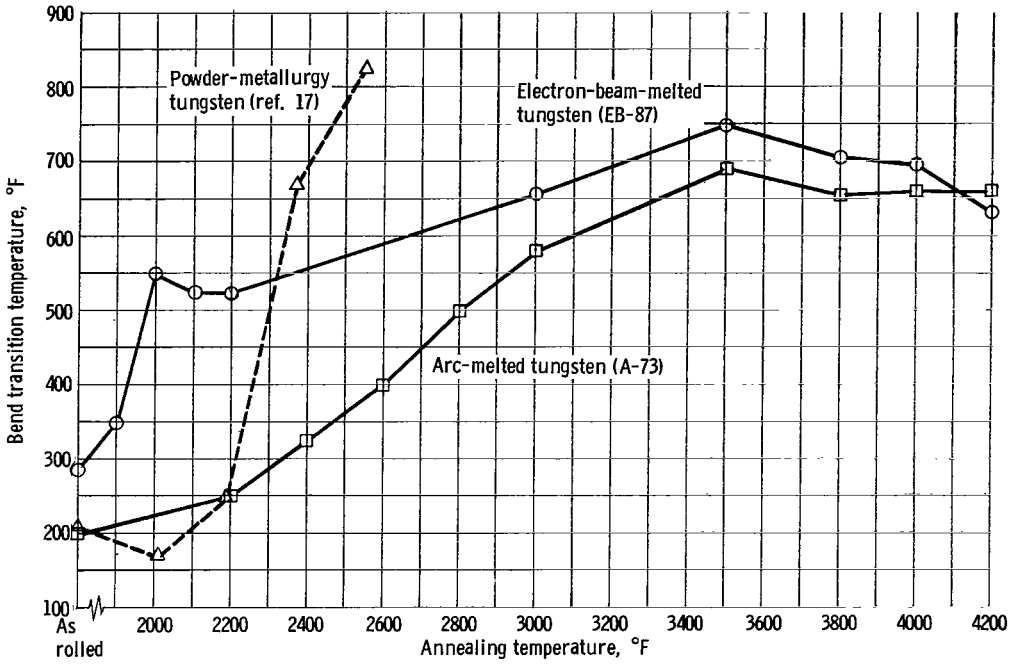

Figure 5. - Bend transition temperature of electron-beam-melted, arc-melted, and powder-metallurgy tungsten after annealing for 1 hour at various temperatures.

lization temperature. After annealing at higher temperatures, 3000° to 4000° F, the EB-melted material still exhibits a bend transition temperature about 50° F higher than that of the arc-melted material. The decreasing ratio of specimen thickness to grain size apparently is responsible for the decrease in transition temperature after annealing at 3800° to 4200° F. The grain size of the EB-melted material approximates the specimen thickness after these annealing treatments.

In comparison, powder-metallurgy tungsten exhibits a slightly lower transition temperature as rolled than the EB-melted tungsten. However, after annealing at 2370° and 2550° F, the transition temperature for the powder-metallurgy material is higher than that of either the EB-melted or the arc-melted materials.

High-Temperature Tensile Properties

Tensile properties of the three lots of EB-melted tungsten are presented in table IX. Tensile properties of one lot of arc-melted tungsten (A-73) tested in sheet form for comparison with EB-87 are also included in this table. The high-temperature ultimate tensile strengths of two lots of annealed EB-melted tungsten tested in rod form are compared in figure 6 with arc-melted tungsten (ref. 1) tested similarly.

It is seen from figure 6 that the strengths of the EB-melted tungsten are substantially lower at high temperatures than that of arc-melted tungsten. The average strength of EB-melted tungsten over the temperature range 2500°

TABLE IX. - TENSILE PROPERTIES OF ELECTRON-BEAM-MELTED AND ARC-MELTED TUNGSTEN AT 2500° TO 4000° F

Test temperature, °F	Annealing condition		0.2 Percent offset yield strength, psi	Ultimate tensile strength, UTS, psi	Elongation, percent	Reduction in area, percent	Strain-hardening coefficient, X, psi^2	Average grain diameter, L, cm
	Time, hr	Temperature, °F						
Lot EB-43 (rod, EB melted)								
2500	1	3600	5 580	16 200	59.4	>95	6.5×10^8	0.0644
3000	1	3600	3 750	10 300	75.2	>95	3.1	.0992
3500	1	3600	960	6 210	66.7	>95	1.3	.127
Lot EB-100 (rod, EB melted)								
2500	As swaged		5 240	16 750	54.6	>95	----	0.0304
	1	2500	5 050	17 100	61.2	>95	12×10^8	0.0166
	1	3600	2 160	12 850	30.5	>95	8.4	.188
3000	As swaged		2 550	11 120	57.6	>95	7.7×10^8	0.0262
	1	3600	1 570	7 250	25.2	>95	4.7×10^8	[a]0.185
3500	As swaged		860	6 220	55.9	>95	1.6×10^8	0.129
	1	3600	990	5 870	35.6	>95	2.2×10^8	0.183
4000	As swaged		790	3 875	65.8	>95	0.98×10^8	0.225
Lot EB-87 (sheet, EB melted)								
2500	As rolled		4 540	18 500	65.2	---	----	(b)
	1	3600	4 060	18 300	72.7	---	16×10^8	0.00566
3000	As rolled		3 910	13 100	80.6	---	7.1×10^8	0.00653
3500	As rolled		3 780	10 300	61.0	---	4.5×10^8	0.00863
Lot A-73 (sheet, arc melted)								
2500	As rolled		40 900	47 400	8.4	---	----	(b)
	1	3600	6 100	22 000	49.9	---	22×10^8	0.00495
3500	1	3600	4 010	8 960	65.0	---	2.5×10^8	0.0165

[a]Estimated grain size.

[b]Wrought.

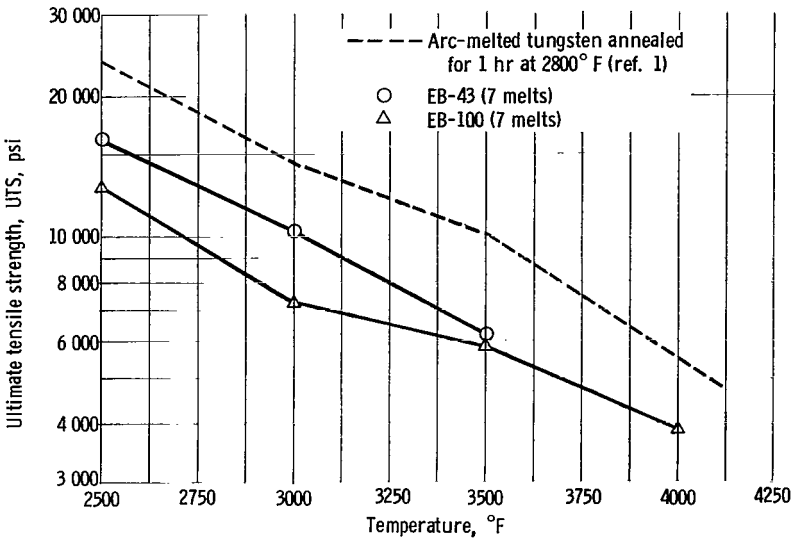

Figure 6. - Ultimate tensile strength of electron-beam-melted tungsten (annealed at 3600° F) and arc-melted tungsten (annealed at 2800° F) at 2500° to 4140° F.

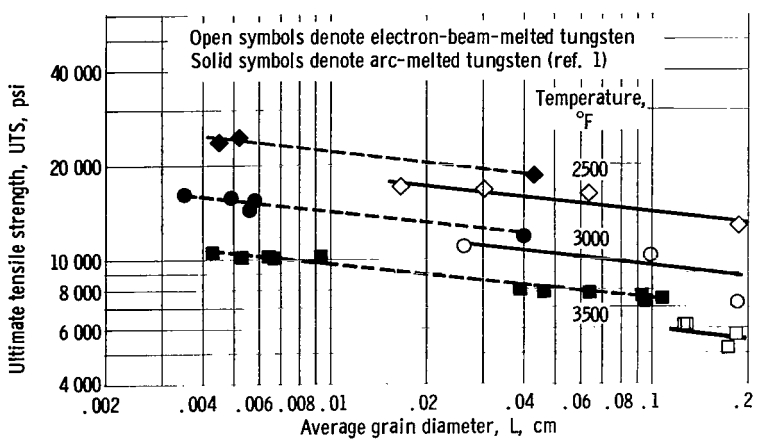

Figure 7. - Effect of grain size on ultimate tensile strength of electron-beam- and arc-melted tungsten at 2500° to 3500° F.

to 4000° F is about 60 percent of the strength of the arc-melted tungsten. Examination of the data in table IX suggests that a correlation can be drawn between the strengths of the various lots of EB-melted tungsten and their microstructures. Those lots with a large grain size (as measured in the specimen shoulder after testing) were weaker than the lots that were not as large grained. This trend has also been documented recently (ref. 1) for arc-melted tungsten. The correlation between ultimate tensile strength and grain size is shown in figure 7. Also included are data for arc-melted tungsten from reference 1. The grain-size dependencies of the two types of materials appear to be similar and do not appear to vary with temperature over the range 2500° to 3500° F. This relation may be expressed by the general relation

$$UTS = AL^{c} \tag{6}$$

where c is a constant determined to be -0.12.

It is also apparent from figure 7 that the ultimate strengths of the EB-melted materials were only about 85 percent as high as the ultimate strength of arc-melted tungsten at the same grain sizes. It is believed that this difference reflects the differences in purity between the two types of materials.

Considerable scatter was observed in the yield strength data for EB-melted tungsten, and these data could not be fitted to a straight-line relation with grain size. The yield strengths were considerably below those reported for arc-melted tungsten in reference 1.

Approximate true-stress - true-strain curves were constructed from the tensile curves for the recrystallized materials to obtain the parabolic strain-hardening coefficients (refs. 18 and 19) from the relation

$$\chi = \frac{(\sigma - \sigma_o)^2}{\epsilon} \tag{7}$$

Representative true-stress - true-strain curves at a crosshead speed of 0.05 inch per minute are shown in figure 8, and parabolic plots of the same curves are shown in figure 9. The data at 3000° F give a good fit to the parabolic relation, while the 2500° and 3500° F data show minor deviations.

The strain-hardening coefficients decreased with increasing temperature, as expected, and also decreased with increasing grain size, as illustrated in figure 10. In comparison with previous data on the strain-hardening

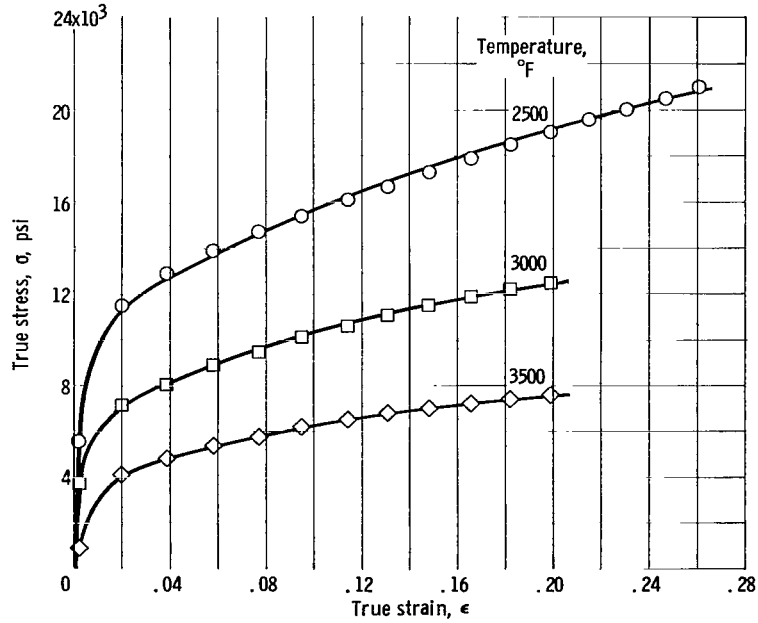

Figure 8. - Effect of temperature on tensile flow curves of electron-beam-melted tungsten at 2500° to 3500° F (lot EB-43, annealed for 1 hr at 3600° F).

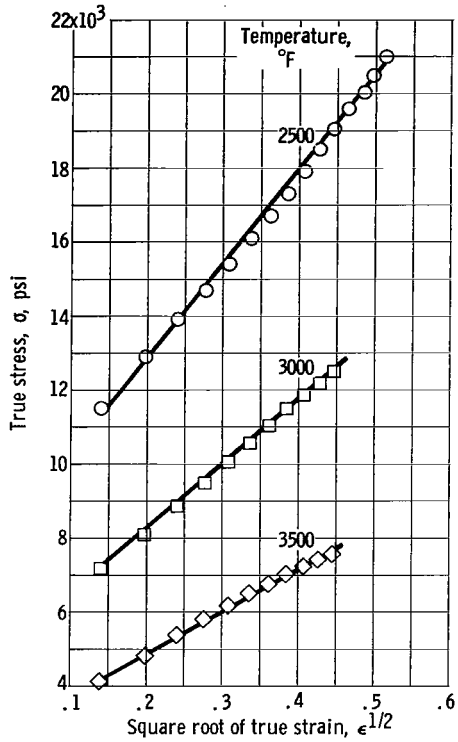

Figure 9. - Parabolic plot of tensile flow curves for electron-beam-melted tungsten at 2500° to 3500° F (lot EB-43, annealed for 1 hr at 3600° F).

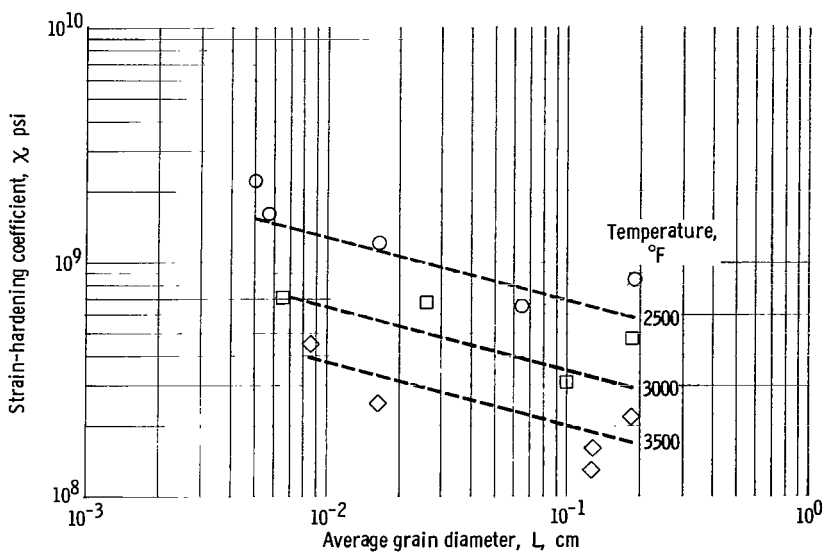

Figure 10. - Effect of grain size on strain-hardening coefficient of electron-beam-melted tungsten at 2500° to 3500° F.

TABLE X. - CREEP DATA FOR ELECTRON-BEAM-MELTED TUNGSTEN

Annealing condition		Test temperature, °F	Stress, S, psi	Transient creep constant, β, $sec^{-1/3}$	Steady creep rate, $\dot{\epsilon}$, sec^{-1}	Average grain diameter, L, cm
Time, hr	Temperature, °F					
Lot EB-43						
1	3600	3500	2130	0.877×10^{-3}	0.373×10^{-6}	----
			4760	12.9×10^{-3}	80.0×10^{-6}	0.42
Lot EB-100						
0.5	3000	2500	4660	0.438×10^{-3}	----	0.038
			5760	1.13	----	
			6870	1.71	----	
As swaged		3000	4010	(a)	----	0.088
			4860	----	4.68×10^{-6}	
		3500	2430	1.46×10^{-3}	0.675×10^{-6}	0.223
			2820	----	1.83	
			3185	----	3.89	
			3675	----	9.79	
			4165	----	21.0	
1	3600	2250	6200	0.786×10^{-3}	----	0.203
		2500		2.56	----	
		2750		4.48	----	
		2750	4220	1.47×10^{-3}	----	0.176
		2875		2.42	0.808×10^{-6}	
		3000		----	1.70	
		3125		----	3.50	
		3250		----	9.81	
		3525	3200	4.36×10^{-3}	5.43×10^{-6}	0.181
		3630		----	1.81	
		3355		----	1.65	
		3495		----	5.51	

[a]Abnormal behavior.

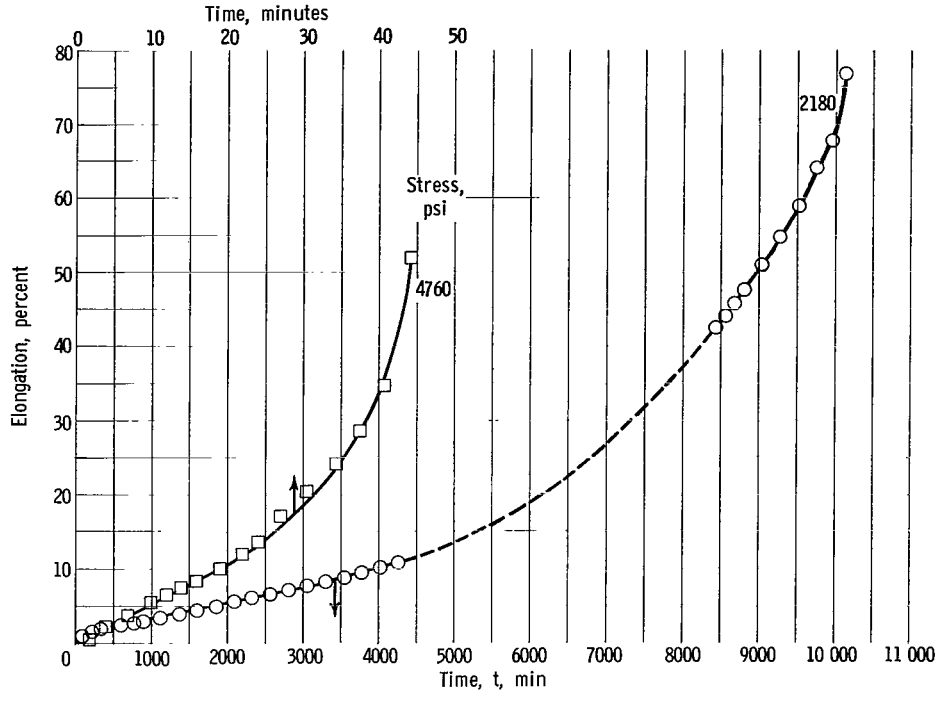

Figure 11. - Constant-load creep curves for electron-beam-melted tungsten at 3500° F.

coefficents for arc-melted tungsten (ref. 1), the coefficents for EB-melted tungsten are only about 70 percent as large when compared at the same temperatures and grain sizes. This difference in flow strength further reflects the difference in purity between the two materials.

High-Temperature Creep-Rupture Properties

Constant-load creep-rupture tests were conducted on lot EB-43 at 3500° F and step-load creep tests were conducted on lot EB-100 at 2250° to 3630° F. Data from these tests are summarized in table X. Representative constant-load creep curves for lot EB-43 at 3500° F are shown in figure 11.

The creep of tungsten at this temperature may be represented by periods of transient or primary creep, during which the creep rate decreases; steady or secondary creep, during which the creep rate is essentially constant; and tertiary creep, characterized by an increasing creep rate terminating in fracture. At 2750° F and lower and at stresses of 4220 to 6870 pounds per square inch, only transient creep was observed prior to tertiary creep; while at 2875° F and higher, both transient and steady creep were observed.

It was shown earlier (ref. 1) that the steady creep rates of arc-melted tungsten could be correlated with stress and grain size by a relation of the form originally suggested by Sherby (ref. 20):

$$\dot{e} = kS^aL^b \qquad (8)$$

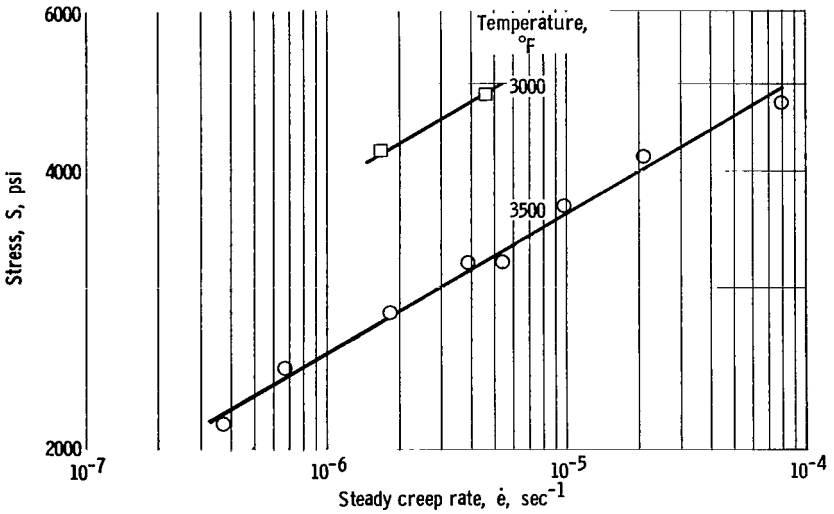

Figure 12. - Steady creep rate plotted against stress for electron-beam-melted tungsten.

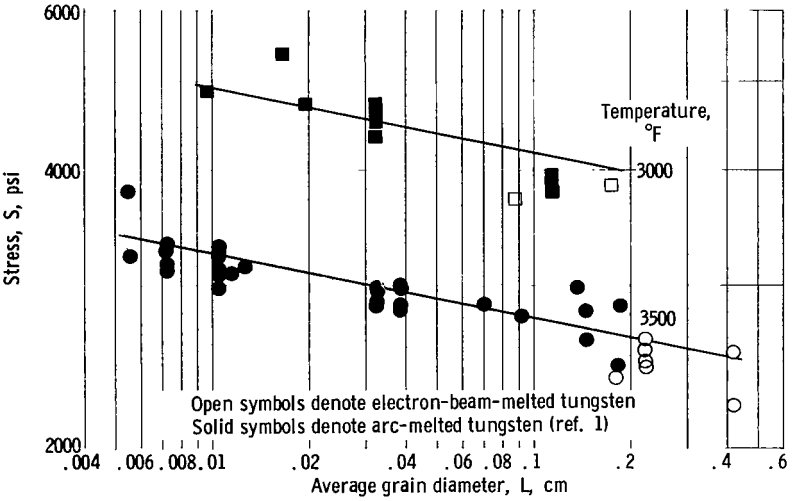

Figure 13. - Grain-size dependency of stress for steady creep rate of 10^{-6} per second.

The average values determined for arc-melted tungsten for the exponential stress factor a and the exponential grain-size factor b were 5.8 and 0.43, respectively.

Figure 12 shows a plot of the steady creep rates at 3000° and 3500° F for EB-melted tungsten against stress. The stress dependency for linear creep of EB-melted tungsten is calculated from this plot as 6.7, higher than the 5.8 observed for arc-melted tungsten.

Figure 13 shows the stress to give a creep rate of 10^{-6} $second^{-1}$ plotted against grain size for both EB- and arc-melted tungsten. Since the data for arc-melted tungsten are more extensive, a stress dependency factor of 5.8 was used in calculating the stress values for this plot. It is seen that the

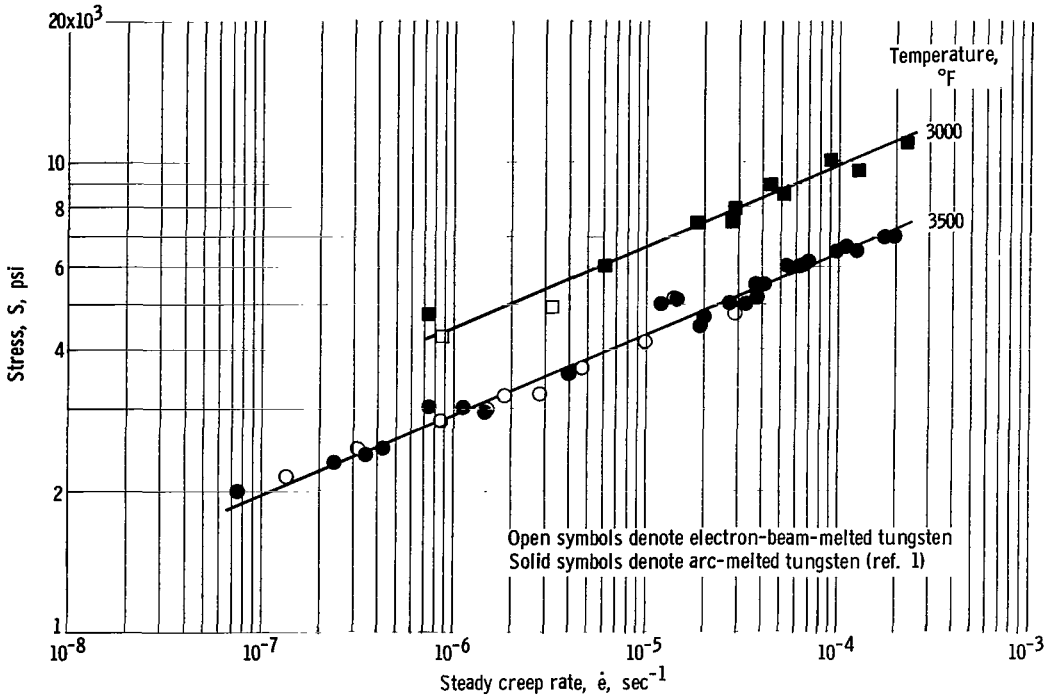

Figure 14. - Steady creep rate as function of stress, normalized to grain size of 0.04 centimeter.

grain-size factor of 0.43 determined for arc-melted tungsten also fits the data for EB-melted tungsten moderately well and that the creep rates for both materials are similar when compared at similar grain sizes.

The creep strength is seen from figure 13 to be proportional to the -0.074 power of grain size, as calculated from equation (8). This is measurably less than the factor of -0.12 observed for the dependency of the short-time ultimate strength on grain size (shown in fig. 7, p. 22), reflecting the probability that there is a change or modification in the rate-controlling reaction. The strength at elevated temperatures is considered to be determined from competition between strain-hardening and recovery reactions. During tensile testing, where the total time is short, strain hardening may exert the predominant influence on strength. During creep testing, however, the test times are considerably longer and recovery reactions are considered rate controlling. The mechanisms by which decreasing grain size is postulated to increase strength are increasing the complexity of slip (ref. 21) and/or increasing the dislocation density (ref. 22). Since these are both associated with strain-hardening rather than recovery, the decrease in grain-size dependence during creep may reflect the increasing importance of recovery as the rate-controlling reaction at low strain rates.

The steady creep rate data at 3000° and 3500° F for EB- and arc-melted tungsten are plotted against stress in figure 14 after normalizing to a grain size of 0.04. The rates were normalized by multiplying each creep rate by the factor $(0.04/L)^{0.43}$ to eliminate variations in the creep rate due to variations in grain size. On this basis, the creep behavior of EB- and arc-melted tungsten

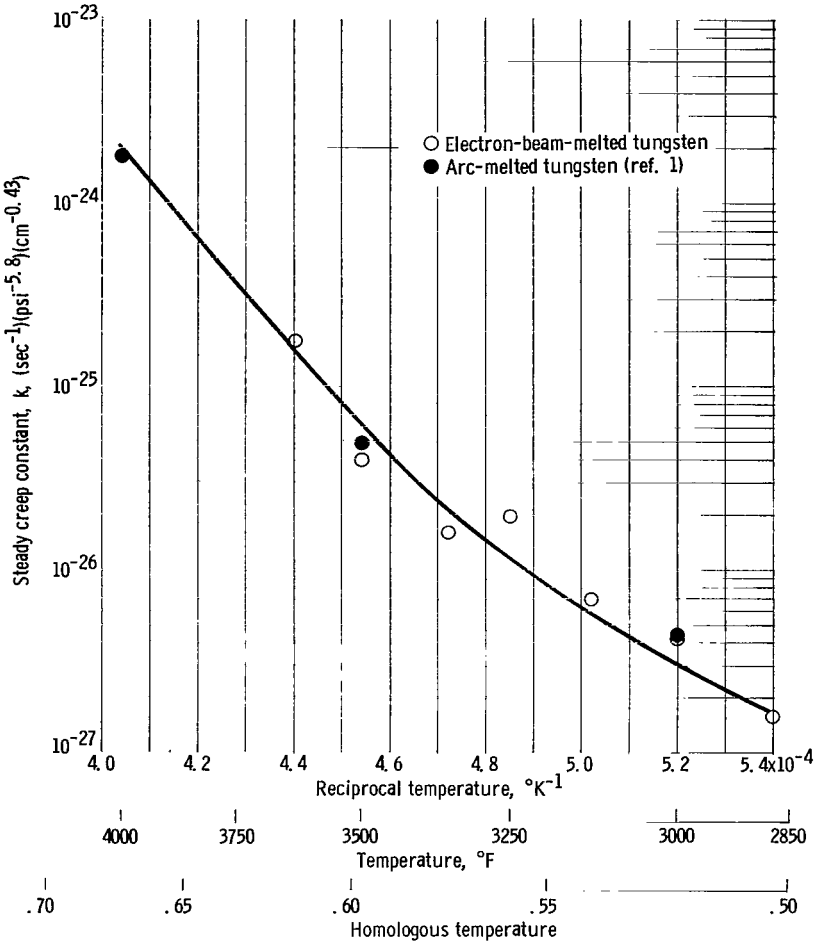

Figure 15. - Temperature dependence of steady creep constant. Activation energy, 141 000±4 000 calories per gram mol.

are seen to be very similar and can be fairly well related using a common stress dependency factor of 5.8.

The temperature dependency of the steady creep constant k, from equation (8), is shown in figure 15. At temperatures above about 3300° F, the temperature dependency corresponds to an activation energy of 141 000±4 000 calories per gram mole, slightly less than the 160 000 calories per gram mole observed by Green (ref. 23). Below about 3300° F, the temperature dependency is seen to decrease.

The activation energy of 141 000 calories per gram mole is close to that for self-diffusion in tungsten, 153 100 calories per gram mole (ref. 14), suggesting that recovery of strain hardening by dislocation climb is the rate-controlling mechanism about 3300° F. The significance of the decrease in activation energy below 3300° F is not entirely clear. However, a similar decrease in the temperature dependency of the steady creep rate of copper in the vicinity of 0.65 T_m has recently been observed by Barrett and Sherby (ref. 24).

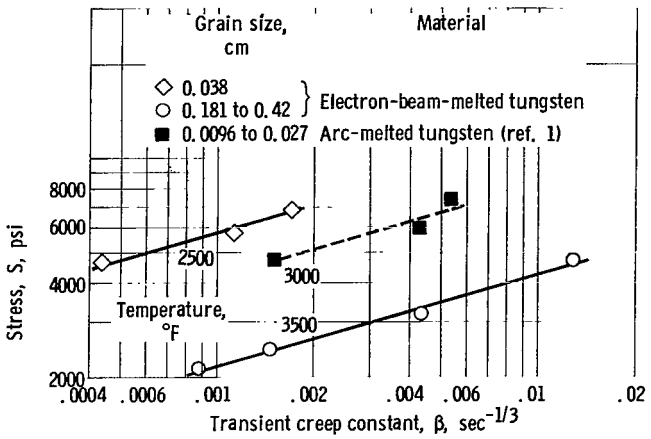

Figure 16. - Transient creep constant as function of stress.

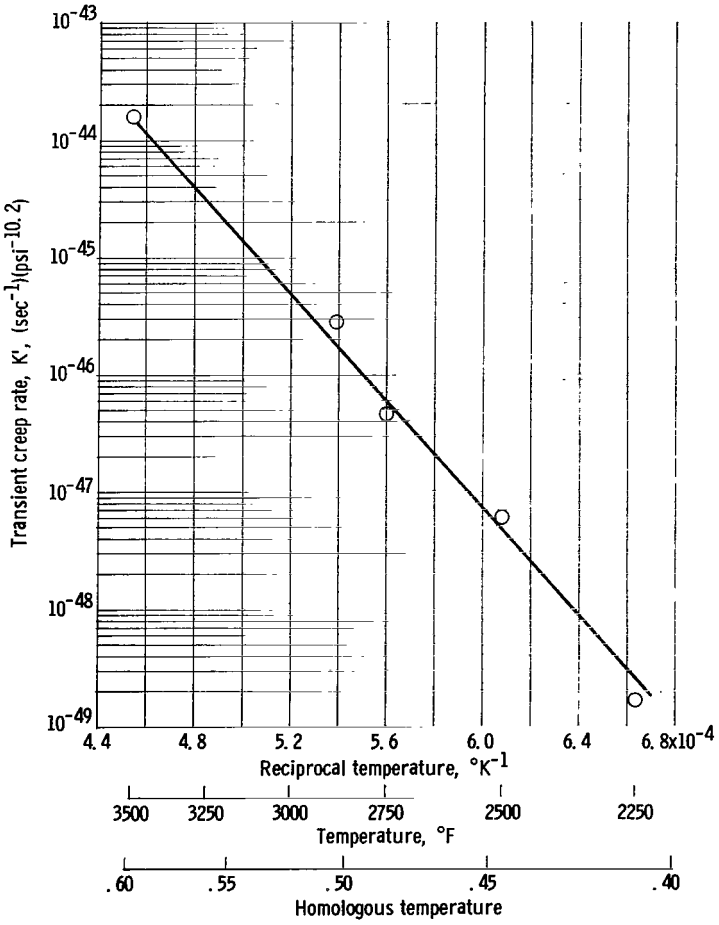

Figure 17. - Temperature dependency of transient creep rate for large-grained electron-beam-melted tungsten. Grain size, 0.092 to 0.42 centimeter; activation energy, 106 400±3 300 calories per gram mol.

These authors suggest that enhanced self-diffusion along dislocation pipes may increase the rate of dislocation climb in this temperature range, resulting in an increased creep rate and nonlinearity of the Arrhenius plot.

The transient or primary creep behavior was also studied at 2250° to 3500° F in order to more completely characterize the high-temperature creep behavior of EB-melted tungsten and to extend the comparison between EB- and arc-melted tungsten. The transient portions of the creep curves for annealed specimens could be correlated according to the familiar Andrade relation

$$e = \beta t^{1/3} \tag{9}$$

Experimentally determined values for the transient creep constant are included in table X (p. 25).

Figure 16 shows the stress dependency of the transient creep constant. Data for materials of similar grain size were selected at each temperature for this plot in order to minimize any effect of grain size on the stress dependency. These data indicate that the transient creep constant varies as the 3.4 power of stress over the temperature range 2500° to 3500° F.

The transient creep constant tended to increase with increasing grain size, as was also noted earlier for the steady creep rate. However, no grain-size dependency was calculated because of the small amount of data on the transient creep constant at different grain sizes.

The temperature dependency of the transient creep rates for large-grained EB-melted tungsten is shown in figure 17. The data over the entire temperature range studied, 2250° to 3500° F, are related by an activation energy of 106 000±3 300 calories per gram mole with no apparent inflections in the curve. Although the linearity of the plot suggests a single rate-controlling mechanism, the mechanism itself cannot yet be described.

Considering the temperature dependencies for transient creep and steady creep of tungsten, the creep behavior of tungsten in the range 2250° (0.41 T_m) to 4000° F (0.67 T_m) may be summarized as follows. It appears that, at least over the temperature range 2250° to 3500° F, creep initially follows the cubic rate law and is controlled by a single, undefined mechanism. At temperatures of 2875° F (0.50 T_m) and higher, the magnitude of activation energy suggests that the strain-hardened structure may be recovered by dislocation climb. Thus, at longer times in this temperature range, complete recovery is possible and steady creep is observed after the initial period of transient (cubic) creep. At 2250° to 2750° F, however, recovery by dislocation climb is so slow that only transient creep is observed before tertiary creep.

CONCLUSIONS

A study has been conducted on the properties of tungsten consolidated by electron-beam-melting, including purity as a function of number of melts, recrystallization and grain growth behavior, low-temperature ductility, and

high-temperature tensile and creep strength.

The following conclusions are drawn:

1. Electron-beam (EB) melting substantially reduces the level of most metallic impurities but not the interstitial impurities in tungsten compared with tungsten consolidated by arc melting. The greatest reductions are in the amounts of aluminum, iron, nickel, and silicon.

2. The rates of strain-induced boundary migration (recrystallization), as calculated from the Johnson-Mehl relation, are higher for EB-melted tungsten than those observed previously for less pure arc-melted tungsten. The average activation energy is approximately 81 000 calories per gram-mole, compared to 104 500 calories per gram-mole for arc-melted tungsten.

3. The rates of grain growth for EB-melted tungsten are higher than those for arc-melted tungsten, further reflecting its higher purity. The activation energies for grain growth ranged from 78 800 to 114 000 calories per gram-mole, suggesting that grain boundary diffusion is the rate-controlling process for both grain growth and recrystallization.

4. The ductile-brittle transition temperatures for EB-melted tungsten, determined in tension and in bending, are similar or slightly higher than those observed for arc-melted and powder-metallurgy tungsten in the worked condition. In the recrystallized condition, the transition temperatures for EB- and arc-melted tungsten are also similar, both being lower than that exhibited by recrystallized powder-metallurgy tungsten of similar grain size.

5. The ultimate tensile strength of EB-melted tungsten at 2500° to 3500° F decreases with increasing grain size, as previously observed for arc-melted tungsten. EB-melted tungsten is about 15 percent weaker in tension than arc-melted tungsten when compared at the same grain size. This difference is ascribed to the difference in purity. The parabolic strain-hardening coefficients for EB-melted tungsten also decreased with increasing grain size.

6. The creep behavior of EB-melted tungsten could be correlated with that observed earlier for arc-melted tungsten. EB-melted tungsten is weaker in creep than arc-melted tungsten because of its larger grain size.

7. The activation energy for steady creep above about 3300° F was 141 000±4 000 calories per gram-mole; from 3300° to 2875° F, it decreased. The magnitude of the activation energy suggests that dislocation climb is rate controlling above 3300° F. The activation energy for transient creep at 2250° to 3500° F was 106 000±3 300 calories per gram-mole; the rate-controlling reaction during transient creep is not known at this time.

Lewis Research Center,
National Aeronautics and Space Administration,
Cleveland, Ohio, October 19, 1965.

REFERENCES

1. Klopp, William D.; and Raffo, Peter L.: Effects of Purity and Structure on Recrystallization, Grain Growth, Ductility, Tensile, and Creep Properties of Arc-Melted Tungsten. NASA TN D-2503, 1964.

2. Witzke, Walter R.; Sutherland, Earl C.; and Watson, Gordon K.: Preliminary Investigation of Melting, Extruding, and Mechanical Properties of Electron-Beam-Melted Tungsten. NASA TN D-1707, 1963.

3. Orehotsky, J. L.; and Steinitz, R.: The Effect of Zone Purification on the Transition Temperature of Polycrystalline Tungsten. Trans. AIME, vol. 224, 1962, pp. 556-560.

4. Campbell, R. W.; and Dickinson, C. D.: Effect of Melting Variables on Purity and Properties of Tungsten. Vol. 18, Pt. 2 of High Temperature Materials, G. M. Ault, W. F. Barclay, and H. P. Munger, eds., Intersci. Pub., Inc., 1963, pp. 655-668.

5. Anon.: Standard Methods for Estimating the Average Grain Size of Metals. ASTM Standards, Pt. 3, ASTM, 1961.

6. Sikora, Paul F.; and Hall, Robert W.: High-Temperature Tensile Properties of Wrought Sintered Tungsten. NASA TN D-79, 1959.

7. Koo, R. C.: Effect of Purity on the Tensile Properties of Tungsten Single Crystals from -196° C to 29° C. Acta Met., vol. 11, no. 9, Sept. 1963, pp. 1083-1095.

8. Drangel, I.; and Murray, G. T.: Parameters Pertinent to Purification by Electron Beam Zone Refinement. Paper Presented at AIME Meeting, New York (N.Y.), Feb. 16-20, 1964.

9. Burke, J. E.; and Turnbull, D.: Recrystallization and Grain Growth. Vol. 3 of Prog. in Metal Phys., Pergamon Press, Inc., 1952, pp. 220-292.

10. English, A. T.; and Backofen, W. A.: Recrystallization in Hot-Worked Silicon-Iron. Trans. AIME, vol. 230, Apr. 1964, pp. 396-407.

11. Detert, Klaus; and Dressler, Gerd: Recrystallization in High-Purity Nickel. Paper Presented at AIME Meeting, Chicago (Ill.), Feb. 14-18, 1965.

12. Feltham, P.; and Copley, G. J.: Grain-Growth in α-Brasses. Acta Met., vol. 6, no. 8, Aug. 1958, pp. 539-542.

13. Cole, D. G.; Feltham, P.; and Gillam, E.: On the Mechanism of Grain Growth in Metals, with Special Reference to Steel. Proc. Phys. Soc. (London), sec. B, vol. 67, Feb. 1954, pp. 131-137.

14. Andelin, R. L.; Knight, J. D.; and Kahn, M.: Diffusion of Tungsten and Rhenium Tracers in Tungsten. Trans. AIME, vol. 233, Jan. 1965, pp. 19-24.

15. Pugh, J. W.: On the Recovery and Recrystallization of Tungsten. Plansee Proc. 1958, F. Benesovsky, ed., 1959, pp. 97-107.

16. Feltham, P.: Grain Growth in Metals. Acta Met., vol. 5, no. 2, Feb. 1957, pp. 97-105.

17. Ogden, H. R.: Department of Defense Refractory Metals Sheet-Rolling Program. Rept. No. DMIC-176, Status Rept. 2, Defense Metals Info. Center, Oct. 15, 1962.

18. Clarebrough, L. M.; and Hargreaves, M. E.: Work Hardening of Metals. Vol. 8 of Prog. in Metal Phys., Pergamon Press, Inc., 1959, pp. 1-103.

19. Wasilewski, R. J.: On Discontinuous Yield and Plastic Flow in α-Titanium. Trans. ASM, vol. 56, no. 2, June 1963, pp. 221-235.

20. Sherby, Oleg D.: Factors Affecting the High Temperature Strength of Polycrystalline Solids. Acta Met., vol. 10, no. 2, Feb. 1962, pp. 135-147.

21. McLean, D.: Mechanical Properties of Metals. John Wiley & Sons, Inc., 1962, pp. 122-124; 285-334.

22. Garofalo, F.; Domis, W. F.; and von Gemmingen, F.:. Effect of Grain Size on the Creep Behavior of an Austenitic Iron-Base Alloy. Trans. AIME, vol. 230, Oct. 1964, pp. 1460-1467.

23. Green, Walter V.: Short-Time Creep-Rupture Behavior of Tungsten at 2250° to 2800° C. Trans. AIME, vol. 215, Dec. 1959, pp. 1057-1060.

24. Barrett, Craig R.; and Sherby, Oleg D.: Steady-State Creep Characteristics of Polycrystalline Copper in the Temperature Range 400° to 950° C. Trans. AIME, vol. 230, Oct. 1964, pp. 1322-1327.

"The aeronautical and space activities of the United States shall be conducted so as to contribute . . . to the expansion of human knowledge of phenomena in the atmosphere and space. The Administration shall provide for the widest practicable and appropriate dissemination of information concerning its activities and the results thereof."

—NATIONAL AERONAUTICS AND SPACE ACT OF 1958

NASA SCIENTIFIC AND TECHNICAL PUBLICATIONS

TECHNICAL REPORTS: Scientific and technical information considered important, complete, and a lasting contribution to existing knowledge.

TECHNICAL NOTES: Information less broad in scope but nevertheless of importance as a contribution to existing knowledge.

TECHNICAL MEMORANDUMS: Information receiving limited distribution because of preliminary data, security classification, or other reasons.

CONTRACTOR REPORTS: Technical information generated in connection with a NASA contract or grant and released under NASA auspices.

TECHNICAL TRANSLATIONS: Information published in a foreign language considered to merit NASA distribution in English.

TECHNICAL REPRINTS: Information derived from NASA activities and initially published in the form of journal articles.

SPECIAL PUBLICATIONS: Information derived from or of value to NASA activities but not necessarily reporting the results of individual NASA-programmed scientific efforts. Publications include conference proceedings, monographs, data compilations, handbooks, sourcebooks, and special bibliographies.

Details on the availability of these publications may be obtained from:

SCIENTIFIC AND TECHNICAL INFORMATION DIVISION

NATIONAL AERONAUTICS AND SPACE ADMINISTRATION

Washington, D.C. 20546